16th European Signal Processing Conference (EUSIPCO 2008), Lausanne, Switzerland, August 25-29, 2008, copyright by EURASIP

MIMO Radar Exploiting Narrowband Frequency-Hopping Waveforms

Yimin Zhang and Moeness Amin

Center for Advanced Communications
Villanova University, Villanova, PA 19085, USA
E-mail: {yimin.zhang, moeness.amin}@villanova.edu

Abstract - Accurate estimation and tracking of the position of moving targets is an important task in urban sensing operations. Dual-frequency radar, which estimates the range of a target based on the phase difference between two closely spaced frequencies, has been shown to be a cost-effective method to accomplish range-to-motion estimation and tracking. Target positioning can be achieved by using multiple dual-frequency radar antennas, either coherently or noncoherenly processed. The dual-frequency radar concept has been extended to develop narrowband (NB) frequency-hopping (FH) radar which, while inherits the advantages of dual-frequency radars, spreads the power over a bandwidth and thereby reduces the signal visibility, probability of intercept, and interference to/from other systems. In this paper, we consider MIMO radar systems that use NB-FH signals to achieve effective positioning of moving/vibrating targets with a small array aperture.

1. INTRODUCTION

Through-the-wall sensing has attracted considerable interest in various civilian and military applications over the recent years. One of the applications is surveillance and reconnaissance in urban environments to estimate the layout of the building and detect and localize moving and vibrating targets behind a wall. While the former often relies on the use of wideband signal to achieve high-resolution imaging, dual-frequency radar has shown to provide good localization and tracking of moving target [1-3]. A dual-frequency radar employs narrowband signal processing and thus requires much lower system complexity compared to wideband radar imaging systems. Exploitation of time-frequency processing techniques further allows the separation of multiple moving targets in the time-frequency domain based on their Doppler signatures, and thus enables the tracking of multiple moving targets [4].

Dual-frequency radars, however, have several shortcomings in practice. First, the ambiguity in the range limits the size of detectable area. Second, the high power of the two operating carriers creates significant interference to environment and will increase its detectability by intelligent adversaries and lead to exposure of the radar surveillance operations. To overcome these problems, narrowband (NB) frequency-hopping (FH) radars have been developed for the detection and localization of moving and vibrating targets [5]. By spreading the carrier frequency over a bandwidth, NB-FH radars have several advantages. (1) Unlike conventional wideband radars, the proposed radar system is narrowband and thus can be implemented with much lower complexity. (2) Compared to dual-frequency radar, the NB-FH radar significantly reduces the peak power spectrum density. Accordingly, the NB-FH radar is more covert due to the reduced probability of intercept and probability of detection, and the waveform is more similar to spread spectrum communication signals. (3) The NB-FH radar reduces interference to and from other communication systems and increases the immunity to interference and jamming. (4) It utilizes a range of frequency separations instead of a fixed one, thus can significantly increase the unambiguous range.

NB-FH radars, similar to dual-frequency radars, only provide the range information. To obtain the cross-range information for the localization of a target, multiple collocated NB-FH radars can be used to perform coherent processing for direction-of-arrival (DOA) estimation, whereas widely separated radars can support trilateration through noncoherent processing. Needless to say, a high cross-range resolution often requires a large number of antennas and a large array aperture, particularly when the signal is weak as typically encountered in through-the-wall applications. This is, however, not feasible in practice when portability and cost-effectiveness are of high priority.

MIMO radar is an emerging technology that is attracting the attention of researchers and practitioners (see, for example, [6, 7] and references therein). When the transmit/receive antennas are widely separated, diversity gain can be achieved. On the other hand, MIMO radars with collocated transmit/receive antennas offer improved resolution, better parameter identifiability, and flexible beam pattern design.

In this paper, we consider the use of multi-sensor NB-FH radars for multiple-input multiple-output (MIMO) radar processing. The use of MIMO radar technology allows one to obtain virtual array aperture which is larger than the actual array aperture. In the underlying NB-FH radar system, the use of FH signals makes it convenient to construct multiple sets of orthogonal or quasi-orthogonal signal waveforms. As a result, the proposed MIMO NB-FH radar is cost-effective, portable, and achieves robust and high resolution performance for moving target localization and tracking. For the simplicity of presentation, the effect of wall is not considered in this paper. In practice, the effect of walls can be compensated when the wall parameters are known or can be estimated [8, 9].

The rest of this paper is organized as follows. Section 2 reviews range estimation concept of a moving target using NB-FH radars. The use of time-frequency analysis for a

NB-FH radar is discussed in Section 3. In Section 4, the concept of MIMO radar using NB-FH signal waveforms is introduced for the moving/vibrating target localization. Discussions are made for far-field as well as near-field operation scenarios. Section 5 provides simulation examples to validate the proposed scheme.

2. NB-FH RADAR CONCEPT

As we detailed in [5], consider a NB-FH radar operating at frequencies $f_1(t) = f_{01} + f_{h1}(t)$ and $f_2(t) = f_{02} + f_{h2}(t)$, where f_{01} and f_{02} are the respective baseline frequencies of two carriers, and $f_{h,1}(t)$ and $f_{h,2}(t)$ are the hopping frequencies which take value from $\{0, \Delta f, \ldots, (N_f-1)\Delta f\}$, with $N_f \Delta f$ equaling to the available bandwidth, W. While $f_{h,1}(t)$ and $f_{h,2}(t)$ may take independent values, their separation must adhere to come constraints that ensure a good sensitivity of the phase difference for robust range estimation. We also assume that the hopping frequencies $f_{h,1}(t)$ and $f_{h,2}(t)$ change synchronously at a hopping rate of r_h, and the corresponding hopping period is $T_h=1/r_h$.

The baseband radar return at the two frequencies, after the hopping frequency is compensated, can be expressed as,

$$s_i(t) = \rho_i(t)\exp(-j\phi_i(t)), \quad i = 1,2, \tag{1}$$

where $\rho_i(t)$ and $\phi_i(t)$ are, respectively, the range-dependent amplitude and the phase of the return corresponding to the i-th frequency of operation. If $R(t)$ is the law of motion of the target, then

$$\phi_1(t) = \frac{4\pi f_1(t)R(t)}{c}, \quad \phi_2(t) = \frac{4\pi f_2(t)R(t)}{c}, \tag{2}$$

where c is the velocity of light. The Doppler frequency shift, $f_{D,i}(t)$, is the differential of the corresponding phase, $\phi_i(t)$, and is given by

$$f_{D,i}(t) = \frac{1}{2\pi}\frac{d\phi_i(t)}{dt} = -\frac{2f_i(t)}{c}\frac{dR(t)}{dt}, \quad i = 1,2. \tag{3}$$

In practice, the phase observation is measured modulo 2π. Thus, it is subject to the phase wrap ambiguity

$$\begin{aligned} \phi_1(t) &= \frac{4\pi f_1(t)R(t)}{c} + 2n(t)\pi, \\ \phi_2(t) &= \frac{4\pi f_2(t)R(t)}{c} + 2m(t)\pi, \end{aligned} \tag{4}$$

where $m(t)$ and $n(t)$ are unknown integers. In NB-FH radar systems, because the frequency changes in each hopping period, $m(t)$ and $n(t)$ also change accordingly in general. Therefore, the range is estimated as

$$\begin{aligned} R(t) &= \frac{c[(\phi_2(t)-\phi_1(t)) - 2\pi(m(t)-n(t))]}{4\pi[f_2(t)-f_1(t)]} \\ &= \frac{c[\phi_2(t)-\phi_1(t)]}{4\pi[f_2(t)-f_1(t)]} - \frac{c[m(t)-n(t)]}{2[f_2(t)-f_1(t)]}. \end{aligned} \tag{5}$$

The second term in the above equation induces ambiguity in range. For specific integers $m(t)$ and $n(t)$, the same phase difference corresponds to infinite range values separated by the following maximum unambiguous range

$$R_{\max}(t) = \frac{c}{2[f_2(t)-f_1(t)]}. \tag{6}$$

While the maximum unambiguous range is an important limiting factor in a dual-frequency radar where the carrier frequencies are fixed, we notice that in the NB-FH radar this carrier frequencies are hopped every hopping period. In other words, the range estimation not only depends on the separation between f_{01} and f_{02}, but also the difference between their respective hopping frequencies, $f_{h,1}(t)$ and $f_{h,2}(t)$, which is assumed to be time-varying. Therefore, the constraint on the carrier frequency separation due to maximum unambiguous range can be relaxed for NB-FH radars, because different values of frequency separation $f_2(t)$–$f_1(t)$ yield distinct $R_{\max}(t)$ at different hopping intervals. Consider that the range changes continuously over the time, such range ambiguity problem can be practically solved by incorporating range estimates over multiple hopping periods in a manner similar to that described in [10]. The combination of hopping frequencies with wide and narrow separation between $f_1(t)$ and $f_2(t)$ allows one to obtain a very large unambiguous range, yet achieve high sensitivity to the target movement. On the other hand, the evaluation of range should be performed separately at each hopping period. Fourier transform over a long period becomes inadequate.

3. TIME-FREQUENCY ANALYSIS

It was shown in [4] that a moderate level of noise may yield significant phase perturbation in a dual-frequency radar and make the phase-based range estimation impractical. Rather, the use of time-frequency representations of the received signal provides robust phase estimation in a highly noisy environment. In addition, time-frequency analysis allows one to separate multiple targets in the time-frequency if they have distinct Doppler signatures. As such, the use of time-frequency analysis tools brings the dual-frequency radar from a conceptual framework into practical platform for the estimation of multiple moving targets in a realistic environment.

The application of time-frequency analysis, for example, the short-time Fourier transform (STFT), to a dual-frequency radar system is relatively straightforward. For fixed carrier frequencies, the STFT of the received signal at each frequency can be computed to depict the signal energy concentration around the true Doppler signatures. It can be shown that the phase information of a signal is preserved at the corresponding peak of the STFT signature with significantly enhanced robustness [11]. Thus, by evaluating the phase difference at the selected autoterm time-frequency points, improved range estimation can be achieved.

In NB-FH radars, however, the phase information is lost in the time-frequency domain if the STFT window spans multiple hopping periods. In particular, when the hopping frequencies of the two carriers change randomly, range estimation from the phase difference between autoterm time-frequency points becomes inadequate. By performing STFT using a window that spans a relatively large number of frequency bins, the mean Doppler signature with respect to the center carrier frequency can be

approximately obtained. Then, robust and accurate phase information can be obtained from the integral of Doppler frequency, as can be easily derived from (3) [4]. The selection of the Doppler signatures in the time-frequency domain, in general, can be achieved using simple peak detection. Kalman filter can also be used to improve the Doppler and range estimation performance [12]. When multiple signal returns exist, some additional work is required to associate different Doppler signatures to different targets. This can be done through segmented strategy and by preserving the phase continuity [13].

4. MIMO NB-FH RADARS

A single-sensor NB FH radar may provide accurate range tracking of moving targets, but it does not uniquely localize the position of these targets because it does not provide cross-range information. Array processing provides the spatial dimensionality to achieve the spatial resolution. As we discussed earlier, the use of MIMO radar concept will further allows one to obtain a virtual array aperture for compact and flexible system design. While the proposed MIMO NB-FH radars can be used for both monostatic and bistatic applications, we consider monostatic radar system in this paper for the convenience of field operation. The radar antennas are collocated and a uniform linear array consisting of M closely spaced antennas is assumed.

The FH signal transmitted from the mth antenna can be expressed as

$$x_i^{[m]}(t) = r^{[m]} \exp[-j2\pi f_i^{[m]}(t)t], \tag{7}$$

where i=1, 2, and the superscript $^{[m]}$ is used to emphasize the signal transmitted from the mth antenna. Furthermore, $r^{[m]}$ in the above expression is a complex scalar representing the amplitude and constant phase of the transmitted signal. The difference of $r^{[m]}$ corresponding to two carrier frequencies is ignored for notational simplicity because of the small frequency separation between them.

When there is a moving target, located at $R(t)$ and the DOA of the target with respect to the array axis is $\theta(t)$. Thus, the signal return, received at the lth antenna, can be expressed as

$$y_{r,i}^{[l,m]}(t) = g^{[l,m]}(t) r^{[m]} \exp[-j2\pi f_i^{[m]}(t)(t - \tau^{[l,m]}(t))], \tag{8}$$

where $g^{[l,m]}(t)$ denotes the return loss and $\tau^{[l,m]}(t)$ denotes the time delay. Both are closely related to the two-way propagation distance.

4.1 Far-Field Scenario

For far-field operation scenarios, such as when the radar is placed with a large standoff distance, the return loss can be considered sensor independent, and the delay can be represented using that evaluated at the reference antenna shifted by an appropriate phase factor. That is,

$$\begin{aligned} y_{r,i}^{[l,m]}(t) = g(t) r^{[m]} \exp[-j2\pi f_i^{[m]}(t)[t - \tau(t)]] \\ \cdot \exp[j2\pi f_i^{[m]}(t) \cdot (l + m - 2)(d/c)\sin\theta(t)], \end{aligned} \tag{9}$$

where $g(t)$ and $\tau(t)$ respectively denote the return loss and phase delay at the reference antenna, which is assumed to be the first antenna, and d is the interelement spacing. Thus, by down converting the received signal into the baseband signal, we obtain

$$y_i^{[l,m]}(t) = g(t) r^{[m]} \exp[j2\pi f_i^{[m]}(t) \cdot (l + m - 2)(d/c)\sin\theta(t)] \tag{10}$$

Therefore, the baseband array signal vector, $\mathbf{y}_i^{[:,m]}(t)$, received at all the M antenna elements corresponding to the signal transmitted from the mth antenna, can be expressed as

$$\mathbf{y}_i^{[:,m]}(t) = g(t) r^{[m]} \mathbf{a}_i^{[:,m]}(t) \exp[j2\pi f_i^{[m]}(t) \cdot (m-1)(d/c)\sin\theta(t)] \tag{11}$$

where

$$\mathbf{a}_i^{[:,m]}(t) = \begin{bmatrix} 1 \\ \exp[j2\pi f_i^{[m]}(t)(d/c)\sin\theta(t)] \\ \vdots \\ \exp[j2\pi f_i^{[m]}(t)(M-1)(d/c)\sin\theta(t)] \end{bmatrix} \tag{12}$$

is the receive steering vector of the array corresponding to operating frequency $f_i^{[m]}(t)$. It emphasized that, unlike a typical MIMO radar application scenario that assumes the same carrier frequency for all the transmit antennas, the receive steering vector depicted in (12) is transmit antenna dependent.

The M antennas can be design to transmit FH waveforms with different hopping frequencies, yielding (quasi-)orthogonal detection at receivers. Stacking the M vectors corresponding to M transmitted waveforms, we obtain the following M^2-dimensional vector

$$\mathbf{y}_i(t) = \begin{bmatrix} \mathbf{y}_i^{[:,1]}(t) \\ \\ \mathbf{y}_i^{[:,M]}(t) \end{bmatrix}. \tag{13}$$

Based on the above receive signal vector, the target can be effectively localized. For far-field operations, each of the M^2 pairs of $\mathbf{y}_1(t)$ and $\mathbf{y}_2(t)$ yields a respective phase difference which is correlated to the same range $R(t)$. As we discussed earlier, the range estimation of each pair can be robustly obtained using time-frequency analysis. While we may need to perform separate STFT for all the pairs, in practice all the received signals are likely to have very close Doppler signature, provided that the window size is properly chosen as we addressed in Section 3. Thus, the autoterm time-frequency point selection only needs to be performed once for each processing block. Nevertheless, averaging the STFT magnitude over different observations enhances the quality Doppler estimates, particularly when the signal is very weak.

Note that, by considering several potential candidates of integers $m(t)$ and $n(t)$, multiple estimates of $R(t)$ can be obtained. Only one of them, which corresponds to the true range, is consistent to that obtained from other pairs. As such, the range ambiguity problem can be solved in each hop interval. The range identifiability can be improved when the frequency separation is designed to follow certain rules (see [10] for example). After the range estimate is

obtained from each pair, these results can be averaged to yield an improved range estimate.

While many DOA estimation methods can be used to find the DOA information, it is often convenient to perform a maximum likelihood (ML) search with respect to θ because we consider a single target here. When multiple targets are involved, they can often be separated in the time-frequency domain for source discrimination [4].

4.2 Near-Field Scenario

For near-field operations, the range and DOA becomes antenna dependent. The range and DOA evaluated at the lth antenna are respectively expressed as

$$R^{[l]}(t) = [R^2(t) + (l-1)^2 d^2 - 2R(t)(l-1)d\sin(\theta(t))]^{1/2} \tag{14}$$

and

$$\theta^{[l]}(t) = \sin^{-1}\left(\frac{R(t)\sin(\theta(t)) - (l-1)d}{[R^2(t) + (l-1)^2 d^2 - 2R(t)(l-1)d\sin(\theta(t))]^{1/2}}\right) \tag{15}$$

In this case, $\tau^{[l,m]}(t)$ is obtained as

$$\begin{aligned}\tau^{[l,m]}(t) &= \tau^{[m]}(t) + \tau^{[l]}(t) \\ &= [R^2(t) + (m-1)^2 d^2 - 2R(t)(m-1)d\sin(\theta(t))]^{1/2}/c \\ &\quad + [R^2(t) + (l-1)^2 d^2 - 2R(t)(l-1)d\sin(\theta(t))]^{1/2}/c.\end{aligned} \tag{16}$$

A vector similar to (11) can be obtained, although it does yield a steering vector with phase term being linear to the array positions. Rather, they are nonlinear and can be approximated using second-order approximations [14].

Similar to the far-field operation scenarios, the range can be first obtained from the $\mathbf{y}_1(t)$ and $\mathbf{y}_2(t)$ pairs. However, in a near-field operation scenario, each pair yields a unique range estimation which depends on l and m. Once the antenna-dependent ranges are estimated, an ML search of θ can be conducted, with the relationship depicted in (14)-(16) considered. Therefore, the complexity is much lower than conventional near-field methods developed for joint range-angle estimations.

5. SIMULATION RESULTS

Two scenarios are considered in this section. The first scenario involves a moving target in the far field, which swings around a center which is 20 m away from the radar. The second scenario involved a vibrating target closely located to the array antennas. For both examples, the hopped carrier frequencies are centered at 1 GHz with a 10 MHz bandwidth. 100 hopping frequency bins are considered, yielding a separation of 100 KHz between two adjacent frequency bins. A four antenna array (M = 4) is used, with an interelement spacing of one wavelength, evaluated at the center of the hopping frequency band, i.e., 1 GHz. Thus, the array aperture is 90 cm. The interelement spacing is chosen to be larger than half-wavelength so as to achieve a large aperture within the portable size. In this case, the array pattern may have grating lobes. In practice, this problem can be mitigated using directional antennas. The frequencies are randomly hopped in each antenna. However, constraints are added to ensure a minimum separation of 2MHz between a pair of frequencies transmitted from each antenna to maintain the phase sensitivity to the range, and a minimum separation of 1 MHz between any of the M^2 frequency combinations at a hopping interval to reduce the interference between the signals transmitted from different antennas.

For the first example, the hopping rate is chosen to be 2 KHz. The observation period is 2 second. In this example, the reflection coefficient is assumed to be a constant, regardless of the range. The input SNR is -5 dB. Fig. 2(a) shows the STFT magnitude of the signal transmitted from and received at the reference antenna, averaged over the two frequencies. The sampling frequency is 10 kHz, and a 2048-point Hanning window is used. Despite the low SNR level, the Doppler signature is clearly identified. Fig. 2(b) shows the range estimation using a single NB-FH radar. Doppler frequency based method [4] is used for the range estimation. With the range estimation alone, however, the cross-range information is missing.

With the use of MIMO radar techniques, the 4-element array allows one to obtain significantly improved Doppler signature by averaging over the combinations with different transmit and receive antennas. The averaged STFT magnitude is shown in Fig. 2(c). The tracked location of the target is depicted in Fig. 2(d).

In the second example, we consider a fan with metallic blades, rotating at 5 cycles/sec (yielding 20 Hz equivalent frequency with 4 blades), and the blade tip is 20 cm from the center. The carrier frequencies are centered at 1 GHz. 100 hopping frequency bins are considered, yielding a separation of 100 KHz between two adjacent frequency bins. The sampling frequency is 20 kHz, and data of 0.5 second duration is used for estimation. The hopping rate is 1 KHz. Fig. 3(a) shows the geometry of the experiment settings. The coordinate of the fan center is (3, 5) m, and the reference antenna is located at the coordinate origin. The input SNR is 0 dB. Fig. 3(b) shows STFT magnitude for the signal transmitted from and received at the reference antenna. A 512-point Hanning window is used. By performing Fourier transform over the entire observation period, discrete signal spectrum can be obtained and is illustrated in Fig. 3(c). From this result, an accurate estimation of the vibration frequency can be obtained. From 20 independent trials, the mean value of the fan center obtained from the 4-element MIMO NB-FH radar is (3.06, 4.98) m, with a standard deviation of (0.13, 0.13) m. The vibration frequency is consistently estimated as 19.9999 Hz for all the 20 trials.

6. CONCLUSIONS

We have presented the concept of MIMO radar exploiting narrowband (NB) frequency-hopping (FH) waveforms. The principle motivation is to develop a cost-effective, portable, and robust radar system for the localization and tracking of moving/vibrating targets applied in through-the-wall radar operations. The proposed MIMO NB-FH radar systems is much simpler compared to wideband radar systems, and it

outperforms the dual-frequency array radar systems in many ways. The frequency hopping techniques allows the proposed system to be covert and resistant to interference, and mitigate the range ambiguity problem. Furthermore, MIMO radar concept allows high resolution localization of moving/vibrating targets with a lower number of array antennas as well as a reduced array aperture for the convenience of portability. Scenarios in both the near- and far-field operations are considered and the feasibility is confirmed using computer simulations.

REFERENCES

1. F. Ahmad, M. Amin, P. Setlur, "Through-the-wall target localization using dual-frequency CW radars," *SPIE Symp. on Defense and Security,* vol. 6201, Orlando, FL, Apr. 2006.
2. A. Lin and H. Ling, "Three-dimensional tracking of humans using very low-complexity radar," *Electronics Letters*, vol. 42, pp. 1062-1064, Aug. 2006.
3. F. Ahmad, M. G. Amin, and P. D. Zemany, "Performance analysis of dual-frequency CW radars for motion detection and ranging in urban sensing applications," *SPIE Symp. on Defense and Security,* Orlando, FL, Apr. 2007.
4. Y. Zhang, M. G. Amin, and F. Ahmad, "A novel approach for moving multi-target localization using dual frequency radars and time-frequency distributions," *Asilomar Conf. Signals, Systems, and Computers*, Pacific Grove, CA, Nov. 2007.
5. Y. Zhang, M. G. Amin, and F. Ahmad, "Narrowband frequency-hopping radar for the localization of moving and vibrating targets," *SPIE Symp. on Defense and Security*, Orlando, FL, March 2008.
6. E. Fishler, A. Haimovich, R. Blum, D. Chizhik, L. Cimini, and R. Valenzuela, "MIMO radar: an idea whose time has come," *IEEE Radar Conf.*, pp. 71-78, April 2004.
7. J. Li and P. Stoica, "MIMO radar with colocated antennas," *IEEE Signal Proc. Mag.*, vol. 24, pp. 106-114, Sept. 2007.
8. G. Wang, M. G. Amin, and Y. Zhang, "A new approach for target locations in the presence of wall ambiguity," *IEEE Trans. Aerospace Electron. Sys.*, vol. 42, pp. 301-315, Jan. 2006.
9. F. Ahmad, Y. Zhang, and M. G. Amin, "Three-dimensional wideband beamforming for imaging through a single wall," *IEEE Geoscience and Remote Sensing Letters*, vol. 5, 2008.
10. X-G. Xia and G. Wang, "Phase unwrapping and a robust Chinese remainder theorem," *IEEE Signal Processing Letters*, vol. 14, pp. 247-250, April 2007.
11. Y. Zhang, M. G. Amin, and F. Ahmad, "Range estimation of multiple targets using dual-frequency radars and time-frequency signal representations," Technical Report submitted to BAE Systems, May 2007.
12. Y. Zhang, P. Setlur, M. G. Amin, and F. Ahmad, "Application of time-frequency analysis and Kalman filter to range estimation of targets in enclosed structures," *IEEE Radar Conf.*, Rome, Italy, May 2008.
13. A. Jarrot, C. Ioana, C. Gervaise, and A. Quinquis, "A time-frequency characterization framework for signals issued from underwater dispersive environments," *IEEE ICASSP*, Honolulu, HI, April 2007.
14. B. A. Obeidat, Y. Zhang, and M. G. Amin, "Range and DOA estimation of polarized near-field signals using fourth-order statistics," *IEEE ICASSP*, Montreal, Canada, May 2004.

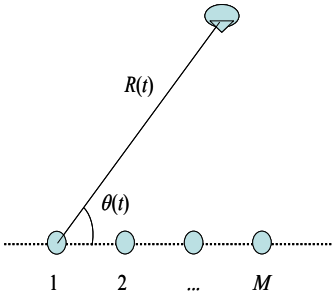

Fig. 1 Array geometry.

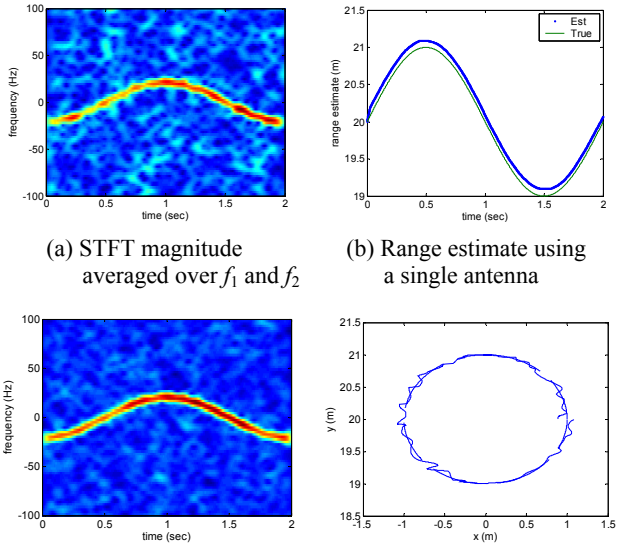

(a) STFT magnitude averaged over f_1 and f_2

(b) Range estimate using a single antenna

(c) STFT magnitude averaged over antennas and frequencies

(d) Location estimation performance

Fig. 2 Far-field moving target case

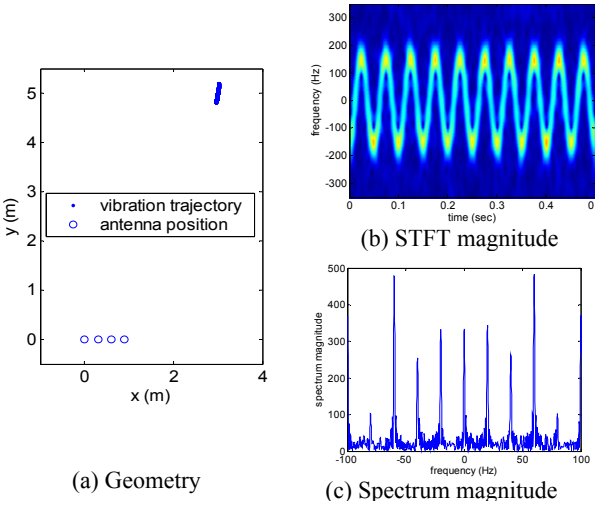

(a) Geometry

(b) STFT magnitude

(c) Spectrum magnitude

Fig. 3 Near-field vibrating target case